Journal of Computational Mathematics
Vol.36, No.1, 2018, 47–69.

http://www.global-sci.org/jcm
doi:10.4208/jcm.1610-m2015-0480

A BIE-BASED DtN-FEM FOR FLUID-SOLID INTERACTION PROBLEMS*

Tao Yin
College of Mathematics and Statistics, Chongqing University, Chongqing 401331, China
Email: taoyin_cqu@163.com
Andreas Rathsfeld
Weierstrass Institute, Mohrenstr. 39, 10117 Berlin, Germany
Email: rathsfeld@wias-berlin.de
Liwei Xu
College of Mathematics and Statistics, Chongqing University, Chongqing 401331, China,
Institute of Computing and Data Sciences, Chongqing University, Chongqing 400044, China
Email: xul@cqu.edu.cn

Abstract

In this paper, we are concerned with the coupling of finite element methods and boundary integral equation methods solving the classical fluid-solid interaction problem in two dimensions. The original transmission problem is reduced to an equivalent nonlocal boundary value problem via introducing a Dirichlet-to-Neumann mapping by the direct boundary integral equation method. We show the existence and uniqueness of the solution for the corresponding variational equation. Numerical results based on the finite element method coupled with the standard Galerkin boundary element method, the fast multipole method and the Nyström method for approximating the DtN mapping are provided to illustrate the efficiency and accuracy of the numerical schemes.

Mathematics subject classification: 65N38, 65N06, 74J05, 76B20.
Key words: Fluid-solid interaction problem, Dirichlet-to-Neumann mapping, Finite element method, Fast multipole method, Nyström method.

1. Introduction

Due to the considerable mathematical and computational challenges such as the oscillating character of solutions and the unbounded domain to be considered, the transmission problems involving acoustic waves scattered by a penetrable elastic body immersed in a fluid have been studied extensively for many years since the pioneering work by Faran [11]. These problems are of great importance in many fields of application including exploration seismology, oceanography, and non-destructive testing, to name a few. In this article, we are interested in the numerical solutions for the two dimensional fluid-solid interaction problem with bounded elastic structure, and we refer to [28] for the variational approach solving the fluid-solid interaction problem over periodic (bi-periodic) structures.

Recently, several numerical methods have been studied for the solution of the fluid-solid interaction problem including the boundary integral equation (BIE) method [31, 39] and its coupling with the finite element method (FEM) [8, 9, 16, 27, 33]. For the coupling scheme, a popular way is to use the BIE methods to solve the acoustic problem outside the obstacle while

* Received December 18, 2015 / Revised version received July 1, 2016 / Accepted October 18, 2016 / Published online October 11, 2017 /

FEM is employed for the approximation of the interior elastic wave. It should be pointed out that any other field equation solver can also be used for solving the interior problem such as the discontinuous Galerkin method [3]. Another approach, the perfectly matched layer (PML) [2], to approximate free radiation is to introduce an additional damping layer surrounding the computational domain such that no reflections occur at its interface with the computational domain. This approach is easy to implement and is very effective. Another way to deal with the fact that the scattered acoustic wave propagates in an unbounded region is to introduce an artificial boundary enclosing the obstacle. Then, after imposing transparent boundary conditions [17] on the artificial boundary, we obtain a reduced nonlocal boundary value problem in a bounded domain which can be solved by field equation solvers. In particular, we can derive a Dirichlet-to-Neumann (DtN) mapping on the artificial boundary to obtain an exact transparent boundary condition, and accordingly this strategy is called DtN method [13]. The DtN mapping can be computed by boundary integral operators [18, 23, 32] or by Fourier-series expansions [12, 38]. The boundary integral equation based (BIE-based) DtN mapping can be defined on any smooth closed curve and this feature may reduce the size of the computational domain, while the Fourier expansion series based DtN mapping is usually defined on a circle or on a perturbation of a circle [34]. In this paper, we are interested in the BIE-based DtN-FEM, and we refer to [38] for the Fourier-series-based DtN-FEM solving the fluid-solid interaction problems.

In contrast to the methods, where the stress tensor is introduced as a main variable [15,16], in this paper the displacement will be the unique unknown in the solid for the fluid-solid interaction problem [4, 27]. Following [32] but using a direct (cf. [26]) instead of an indirect way, we first introduce a nonlocal boundary value problem equivalent to the original problem by representing the exact DtN mapping via the boundary integral operators in acoutics, and then we investigate the existence and uniqueness of the solution for the corresponding variational equation. To compute the DtN mapping, we adopt the standard Galerkin boundary element method (SGBEM), the fast multipole method (FMM) [5,26,36] and the Nyström method (NM), respectively. Actually, if the number of those basis functions of the finite element space which do not vanish on the artificial boundary is N_θ, then we have to solve the BIE N_θ times with different Dirichlet boundary values as right-hand side to approximate the DtN mapping directly. However, following the techniques in [32] we observe that, if the artificial boundary is a circle, then it is sufficient to solve only one BIE with a fixed Dirichlet boundary value. Based on the solution of this BIE, we derive an explicit formulation to compute the sesquilinear form corresponding to the DtN mapping in this case.

The remainder of the paper is organized as follows. We first describe the classical fluid-solid interaction problem in Section 2, and then reduce the transmission problem to a nonlocal boundary value problem by defining a BIE-based DtN mapping in Section 3. Existence and uniqueness of the solution for the corresponding variational equation are discussed in Section 4. In Section 5, we describe the numerical schemes of the FEM and SGBEM, FMM, and NM for solving the boundary integral equation of the first kind. Finally, several numerical tests in Section 6 are presented to verify the efficiency and accuracy of the numerical schemes.

2. The Fluid-solid Interaction Problem

Let $\Omega \subset \mathbb{R}^2$ be an open, bounded, and simply connected domain with a closed and sufficiently smooth boundary $\Gamma = \partial\Omega$, and suppose its exterior complement is given by $\Omega^c = \mathbb{R}^2 \setminus \overline{\Omega} \subset$

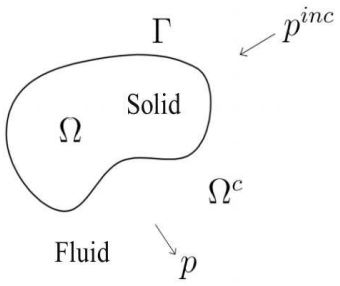

Fig. 2.1. Geometry settings for the boundary value problem (2.1)–(2.5).

$\mathbb{R}^2$. The domain Ω is occupied by a linear and isotropic elastic body, and Ω^c is filled with a homogeneous compressible inviscid fluid of constant mass density. Let p^{inc} be a time-harmonic incident wave. Under the hypothesis of small amplitude oscillations both in the solid and in the fluid, the mathematical description of a direct fluid-solid interaction problem reads: *Given p^{inc}, determine the elastic displacement $\mathbf{u} = (u_1, u_2) \in \left(C^2(\Omega) \cap C^1(\overline{\Omega})\right)^2$ and the acoustic scattered wave $p \in C^2(\Omega^c) \cap C^1(\overline{\Omega^c})$ satisfying*

$$\Delta^* \mathbf{u} + \rho\omega^2 \mathbf{u} = \mathbf{0} \qquad \text{in} \quad \Omega, \tag{2.1}$$

$$\Delta p + k^2 p = 0 \qquad \text{in} \quad \Omega^c, \tag{2.2}$$

$$\omega^2 \rho_f \mathbf{u} \cdot \mathbf{n} = \frac{\partial}{\partial n}(p + p^{inc}) \quad \text{on} \quad \Gamma, \tag{2.3}$$

$$\mathbf{T}\mathbf{u} = -\mathbf{n}(p + p^{inc}) \qquad \text{on} \quad \Gamma, \tag{2.4}$$

and the Sommerfeld radiation condition

$$\lim_{r\to\infty} r^{\frac{1}{2}} \left(\frac{\partial p}{\partial r} - ikp \right) = 0, \quad r = |x|. \tag{2.5}$$

Here, $\omega > 0$ is the frequency, $k = \omega/c_s > 0$ is the acoustic wave number, c_s the speed of sound in the fluid, ρ the density of the solid, ρ_f the density of the fluid, $\partial/\partial n$ the normal derivative on Γ (here and in the sequel, $\mathbf{n}$ is always the outward unit normal to the boundary) and $i = \sqrt{-1}$ the imaginary unit. The operator Δ^* is defined by

$$\Delta^* = \mu\Delta + (\lambda + \mu)\nabla\nabla\cdot\,,$$

where λ, μ are the Lamé constants such that $\mu > 0$ and $\lambda + \mu > 0$, and Δ is the Laplacian. The operator $\nabla\cdot$ is the divergence, and ∇ denotes the gradient. The standard stress operator $\mathbf{T}$ on the boundary is defined by

$$\mathbf{T}\mathbf{u} = 2\mu \frac{\partial \mathbf{u}}{\partial n} + \lambda \mathbf{n} \nabla \cdot \mathbf{u} + \mu \mathbf{n} \times \nabla \times \mathbf{u}.$$

It is known [29] that, for certain geometries and frequencies ω, the problem (2.1)–(2.5) is not always uniquely solvable due to the occurrence of special traction free oscillations. These ω are also known as the Jones frequencies which are inherent to the original model. Here, we call a nontrivial $\mathbf{u}_0$ a traction free solution if it satisfies

$$\Delta^* \mathbf{u}_0 + \rho\omega^2 \mathbf{u}_0 = \mathbf{0} \qquad \text{in} \quad \Omega,$$

$$\mathbf{T}\mathbf{u}_0 = \mathbf{0} \qquad \text{on} \quad \Gamma,$$

$$\mathbf{u}_0 \cdot \mathbf{n} = 0 \qquad \text{on} \quad \Gamma.$$

We conclude from [31] that

Theorem 2.1. *If the surface* Γ *and the material parameters* (μ, λ, ρ) *are such that there are no traction free solutions, then the boundary value problem* (2.1)–(2.5) *has at most one solution.*

To simplify the presentation throughout the paper, we shall denote by $c > 0$, $\alpha > 0$ and $\beta \geq 0$ generic constants whose precise values are not required and may change line by line.

3. Nonlocal Boundary Value Problem

In this section, we derive a nonlocal boundary value problem which is equivalent with the transmission problem (2.1)–(2.5) in a bounded domain. To do so, we introduce a sufficiently smooth artificial boundary Γ_D which is large enough to enclose the entire region Ω. Then the exterior domain Ω^c is decomposed into two subdomains denoted by Ω_D and Ω_D^c, respectively, where Ω_D is the annular region between Γ and Γ_D, and $\Omega_D^c = \mathbb{R}^2 \setminus \overline{\Omega \cup \Omega_D}$ is the unbounded exterior region.

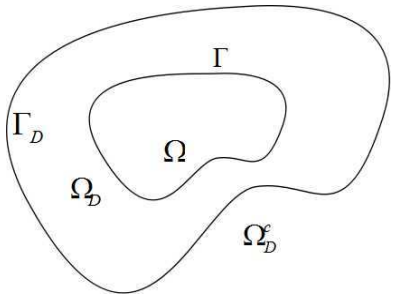

Fig. 3.1. Geometry settings for the nonlocal boundary value problem (3.13)–(3.17).

To impose suitable boundary conditions on Γ_D which are able to capture the nature of the scattering field at infinity, we begin with the transmission conditions on the interface Γ_D

$$[p]_{\Gamma_D} = p_2^+ - p_1^- = 0, \tag{3.1}$$

$$\left[\frac{\partial p}{\partial n}\right]_{\Gamma_D} = \frac{\partial p_2}{\partial n}^+ - \frac{\partial p_1}{\partial n}^- = 0, \tag{3.2}$$

with

$$p(x) = \begin{cases} p_1(x), & x \in \Omega_D, \\ p_2(x), & x \in \Omega_D^c. \end{cases}$$

Here, we write v^- and v^+ for the limits or traces for any functions v on Γ_D from Ω_D and Ω_D^c, respectively. With this partition of the original exterior domain Ω^c, the boundary value problem (2.1)–(2.5) is actually transformed into a transmission problem with an interface Γ_D. In order to eliminate p_2 in Ω_D^c, we now consider the DtN mapping computed via BIE.

3.1. The DtN mapping

To define the DtN mapping on Γ_D, we first consider the following exterior Dirichlet problem: *Given* $p_1^- = p_1|_{\Gamma_D}$, *find* $p_2 \in C^2(\Omega_D^c) \cap C^1(\overline{\Omega_D^c})$ *satisfying*

$$\Delta p_2 + k^2 p_2 = 0 \qquad \text{in} \quad \Omega_D^c, \tag{3.3}$$

$$p_2^+ = p_1^- \qquad \text{on} \quad \Gamma_D, \tag{3.4}$$

$$\lim_{r\to\infty} r^{\frac{1}{2}}\left(\frac{\partial p_2}{\partial r} - ikp_2\right) = 0, \qquad r = |x|. \tag{3.5}$$

We state without proof the following well-known uniqueness result [7].

Theorem 3.1. *The exterior acoustic scattering problem* (3.3)–(3.5) *has at most one solution.*

Now the value of the DtN mapping applied to a function p_1^- on Γ_D is the trace function $(\partial p_2/\partial n)|_{\Gamma_D}$, where p_2 is the solution of (3.3)–(3.5). We shall compute this mapping via boundary integral operators. Let $E(x, y)$ be the fundamental solution of the Helmholtz equation in $\mathbb{R}^2$, that is,

$$E(x,y) = \frac{i}{4}H_0^{(1)}(k|x-y|), \quad x \neq y, \tag{3.6}$$

where $H_0^{(1)}(\cdot)$ is the first kind Hankel function of order zero. Then the classical solution p_2 of the boundary value problem (3.3)–(3.5) can be represented by Green's representation formula as [25]

$$p_2(x) := \int_{\Gamma_D} \frac{\partial E(x,y)}{\partial n_y}\mu(y)ds_y - \int_{\Gamma_D} E(x,y)\sigma(y)ds_y, \quad \forall x \in \Omega_D^c, \tag{3.7}$$

where

$$\sigma(y) = \frac{\partial p_2}{\partial n_y}^+, \quad \mu(y) = p_2^+$$

are called the Cauchy data on Γ_D for the solution p_2. Letting x in (3.7) approach the boundary Γ_D and applying the jump relations, we obtain the BIE which reads:

$$V\sigma(x) = \left(-\frac{I}{2} + K\right)\mu(x), \quad \forall x \in \Gamma_D. \tag{3.8}$$

Here I stands for the identity operator, V and K are the basic simple- and double-layer boundary integral operators defined by

$$V\sigma(x) = \int_{\Gamma_D} E(x,y)\sigma(y)ds_y, \qquad x \in \Gamma_D, \tag{3.9}$$

$$K\mu(x) = \int_{\Gamma_D} \frac{\partial E(x,y)}{\partial n_y}\mu(y)ds_y, \qquad x \in \Gamma_D, \tag{3.10}$$

respectively. From the boundary condition (3.4), we obtain the BIE of the first kind for the unknown σ

$$V\sigma(x) = \left(-\frac{I}{2} + K\right)p_1^-(x) \quad \text{on} \quad \Gamma_D. \tag{3.11}$$

The solution of the BIE (3.11) is not unique for arbitrary wave numbers k because there exist exceptional values k such that $-k^2$ is an eigenvalue of the interior Dirichlet problem for the Laplacian operator inside Γ_D. More precisely, we have the following theorem whose proof can be found in [6].

Theorem 3.2. *For given $\mu = p_1^- \in C^{\alpha+1}(\Gamma_D)$, $0 < \alpha < 1$, the boundary integral equation* (3.11) *is uniquely solvable for $\sigma \in C^\alpha(\Gamma_D)$ provided that k is not an exceptional value.*

Prior to representing the DtN mapping in terms of boundary integral operators, we state without proof some of the important properties [22, 25] for the boundary integral operators V and K on Sobolev spaces $H^s(\Gamma_D), s \in \mathbb{R}$.

Proposition 3.1. *For a sufficiently smooth artificial boundary Γ_D, we have that*

1. *the simple-layer boundary integral operator V is an isomorphism from $H^s(\Gamma_D) \to H^{s+1}(\Gamma_D)$ for all $s \in \mathbb{R}$ provided that the wave number k is not an exceptional value,*

2. *the double-layer boundary integral operator K is a continuous mapping from $H^s(\Gamma_D) \to H^{s+1}(\Gamma_D)$ for all $s \in \mathbb{R}$.*

From the fact that the solution of the BIE (3.11) yields the DtN mapping for p_2 in Ω_D^c, and the transmission conditions for p_1 and p_2 on Γ_D, we know that the solution of the BIE (3.11) also gives a DtN mapping for the boundary data of p_1 in Ω_D. Applying the properties of boundary integral operators V and K, we are now in a position to define an algorithm to compute the DtN mapping $S : H^s(\Gamma_D) \to H^{s-1}(\Gamma_D)$, $1/2 \le s \in \mathbb{R}$, as

$$\frac{\partial \varphi}{\partial n}\Big|_{\Gamma_D} = S\varphi := V^{-1}\left(-\frac{I}{2} + K\right)\varphi, \quad \forall \varphi \in H^s(\Gamma_D). \tag{3.12}$$

Then the condition

$$\frac{\partial {p_1}^-}{\partial n} = S p_1^- \quad \text{on} \quad \Gamma_D$$

in terms of the DtN mapping S could define a nonlocal boundary condition for p_1 on Γ_D.

Theorem 3.3. *The DtN mapping S in* (3.12) *is a bounded linear operator from $H^s(\Gamma_D)$ to $H^{s-1}(\Gamma_D)$ for any $s \ge 1/2$ provided that the wave number k is not exceptional.*

Proof. For all $\varphi \in H^s(\Gamma_D)$ and $s \ge 1/2$ we conclude from Proposition 3.1 that

$$\begin{aligned} &\left\| V^{-1}\left(-\frac{I}{2} + K\right)\varphi \right\|_{H^{s-1}(\Gamma_D)} \\ &\le \left\|V^{-1}\right\| \left\| -\frac{I}{2} + K \right\| \|\varphi\|_{H^s(\Gamma_D)} \le c\|\varphi\|_{H^s(\Gamma_D)}, \end{aligned}$$

where $c > 0$ is a constant independent of φ.

Remark 3.1. The representation of the DtN mapping on Γ_D by boundary integral operators is generally by no means a unique process. Alternatively to our approach, one can employ an indirect method in terms of a potential ansatz [32] to derive the BIE for solving the exterior acoustic scattering problem (3.3)–(3.5). It is worth mentioning that the restriction imposed on the wave number k is technical and is not inherited from the original physical problem. This restriction can be removed using stabilization techniques for the BIE method [10].

3.2. Nonlocal boundary value problem

Using the DtN mapping S in (3.12), the transmission problem (2.1)–(2.5) can be equivalently replaced by the following nonlocal boundary value problem: *Given* p^{inc}, *find* $\mathbf{u} \in \left(C^2(\Omega) \cap C^1(\overline{\Omega})\right)^2$ *and* $p \in C^2(\Omega_D) \cap C^1(\overline{\Omega_D})$ *such that*

$$\Delta^* \mathbf{u} + \rho\omega^2 \mathbf{u} = \mathbf{0} \qquad \text{in} \quad \Omega, \tag{3.13}$$

$$\Delta p + k^2 p = 0 \qquad \text{in} \quad \Omega_D, \tag{3.14}$$

$$\omega^2 \rho_f \mathbf{u} \cdot \mathbf{n} = \frac{\partial}{\partial n}(p + p^{inc}) \qquad \text{on} \quad \Gamma, \tag{3.15}$$

$$\mathbf{T}\mathbf{u} = -\mathbf{n}(p + p^{inc}) \qquad \text{on} \quad \Gamma, \tag{3.16}$$

$$\frac{\partial p}{\partial n} = Sp \qquad \text{on} \quad \Gamma_D, \tag{3.17}$$

where for simplicity, we suppress the subindex 1 for p_1. The following uniqueness result for the problem (3.13)–(3.17) can be easily established.

Theorem 3.4. *If* (a). *the surface* Γ *and the material parameters* (μ, λ, ρ) *are such that there are no traction free solutions, and* (b). *the artificial boundary* Γ_D *is such that* k *is not an exceptional value, then the nonlocal boundary value problem* (3.13)–(3.17) *has at most one solution.*

Proof. It is sufficient to prove that the corresponding homogeneous boundary value problem (3.13)–(3.17) has only the trivial solution. Suppose that $(\mathbf{u}_0, p_0)$ is the solution of the corresponding homogeneous boundary value problem of (3.13)–(3.17). Now let p_1 be the solution of the exterior Dirichlet problem for the Helmholtz equation:

$$\Delta p_1 + k^2 p_1 = 0 \qquad \text{in} \quad \Omega_D^c, \tag{3.18}$$

$$p_1 = p_0 \qquad \text{on} \quad \Gamma_D, \tag{3.19}$$

$$\lim_{r\to\infty} r^{\frac{1}{2}}\left(\frac{\partial p_1}{\partial r} - ikp_1\right) = 0, \qquad r = |x|. \tag{3.20}$$

Then p_1 can be represented as

$$p_1(x) = \int_{\Gamma_D} \frac{\partial E(x,y)}{\partial n_y} \mu_1(y) ds_y - \int_{\Gamma_D} E(x,y)\sigma_1(y) ds_y, \quad \forall x \in \Omega_D^c, \tag{3.21}$$

where $\mu_1 = p_1|_{\Gamma_D}$ and $\sigma_1 = (\partial p_1/\partial n)|_{\Gamma_D}$. Letting x approach Γ_D and employing the jump relations, we obtain the boundary integral equation

$$V\sigma_1(x) = \left(-\frac{I}{2} + K\right)\mu_1(x) \quad \text{on} \quad \Gamma_D.$$

Because of the assumption (b) and the boundary condition (3.19), we have

$$\sigma_1(x) = V^{-1}\left(-\frac{I}{2} + K\right)p_0(x) = Sp_0 \quad \text{on} \quad \Gamma_D.$$

Meanwhile, the nonlocal boundary condition (3.17) on Γ_D leads to $\sigma_0 = Sp_0$, where $\sigma_0 = (\partial p_0/\partial n)|_{\Gamma_D}$. Hence,

$$\sigma_1 = \sigma_0. \tag{3.22}$$

Define the function $(\mathbf{u}, \boldsymbol{p}) \in \big(C^2(\Omega) \cap C^1(\bar{\Omega})\big)^2 \times (C^2(\Omega_D \cup \Omega_D^c) \cap C^1(\overline{\Omega_D}))$ with $\mathbf{u}$ the solution on Ω and $\boldsymbol{p}$ as

$$\boldsymbol{p} = \begin{cases} p_0, & x \in \Omega_D, \\ p_1, & x \in \Omega_D^c. \end{cases}$$

Then by (3.19) and (3.22), we can see that both p and $\partial p/\partial n$ are continuous across the interface Γ_D. Therefore, $(\mathbf{u}, p)$ is the solution of the corresponding homogeneous boundary value problem of (2.1)–(2.5). Then assumption (a) leads to $(\mathbf{u}_0, p_0) = (\mathbf{0}, 0)$. This completes the proof. □

4. Weak Formulation

The standard weak formulation of the nonlocal boundary value problem (3.13)–(3.17) reads: *Given* $\big(p^{inc}, \partial p^{inc}/\partial n\big) \in H^{1/2}(\Gamma) \times H^{-1/2}(\Gamma)$, *find* $\mathbf{U} = (\mathbf{u}, p, p_N) \in \mathcal{H}^1 := \big(H^1(\Omega)\big)^2 \times H^1(\Omega_D) \times H^{-1/2}(\Gamma_D)$ *such that* $\forall\, \mathbf{V} = (\mathbf{v}, q, q_N) \in \mathcal{H}^1$,

$$A(\mathbf{U}, \mathbf{V}) = a_1(\mathbf{u}, \mathbf{v}) + a_2(p, q) + a_3(\mathbf{u}, q) + a_4(p, \mathbf{v}) + b((p, p_N), (q, q_N)) = \ell(\mathbf{V}), \tag{4.1}$$

where

$$a_1(\mathbf{u}, \mathbf{v}) = \int_\Omega \Big[\lambda(\nabla \cdot \mathbf{u})(\nabla \cdot \overline{\mathbf{v}}) + \frac{\mu}{2}\big(\nabla \mathbf{u} + (\nabla \mathbf{u})^T\big) : \big(\nabla \overline{\mathbf{v}} + (\nabla \overline{\mathbf{v}})^T\big) - \rho\omega^2 \mathbf{u} \cdot \overline{\mathbf{v}}\Big]\, dx, \tag{4.2}$$

$$a_2(p, q) = \int_{\Omega_D} \big(\nabla p \cdot \nabla \bar{q} - k^2 p \overline{q}\big)\, dx, \tag{4.3}$$

$$a_3(\mathbf{u}, q) = \rho_f \omega^2 \int_\Gamma \mathbf{u} \cdot \mathbf{n} \overline{q} ds, \quad a_4(p, \mathbf{v}) = \int_\Gamma \mathbf{n} p \cdot \overline{\mathbf{v}} ds, \tag{4.4}$$

$$b\big((p, p_N), (q, q_N)\big) = -2 \int_{\Gamma_D} \Big(-\frac{1}{2} I + K \Big) p\, \overline{q}_N ds + 2 \int_{\Gamma_D} V p_N\, \overline{q}_N ds - \int_{\Gamma_D} p_N \overline{q} ds \tag{4.5}$$

are sesquilinear forms defined on $\big(H^1(\Omega)\big)^2 \times \big(H^1(\Omega)\big)^2$, $H^1(\Omega_D) \times H^1(\Omega_D)$, $\big(H^1(\Omega)\big)^2 \times H^1(\Omega_D)$, $H^1(\Omega_D) \times \big(H^1(\Omega)\big)^2$ and $H^1(\Omega_D) \times H^{-1/2}(\Gamma_D) \times H^1(\Omega_D) \times H^{-1/2}(\Gamma_D)$, respectively, and ℓ defined by

$$\ell(\mathbf{V}) = \int_\Gamma \frac{\partial p^{inc}}{\partial n} \overline{q} ds - \int_\Gamma \mathbf{n} p^{inc} \cdot \overline{\mathbf{v}} ds, \tag{4.6}$$

is a linear functional on $\mathcal{H}^1$ dependent on $\big(p^{inc}, \partial p^{inc}/\partial n\big)$. Here, the norm of $\mathbf{U} = (\mathbf{u}, p, p_N)$ on the product space $\mathcal{H}^t = \big(H^t(\Omega)\big)^2 \times H^t(\Omega_D) \times H^{t-1/2}(\Gamma_D)$ is defined as

$$\|\mathbf{U}\|_{\mathcal{H}^t} = \Big(\|\mathbf{u}\|^2_{(H^t(\Omega))^2} + \|p\|^2_{H^t(\Omega_D)} + \|p_N\|^2_{H^{t-1/2}(\Gamma_D)} \Big)^{1/2}.$$

Remark 4.1. The double dot notation appearing in (4.2) is understood in the following way. If tensors $\mathbf{A}$ and $\mathbf{B}$ have rectangular Cartesian components a_{ij} and b_{ij}, $i, j = 1, \ldots, N$, respectively, then the double contraction of $\mathbf{A} = (a_{ij})$ and $\mathbf{B} = (b_{ij})$ is

$$\mathbf{A} : \mathbf{B} = \sum_{i=1}^N \sum_{j=1}^N a_{ij} b_{ij}. \tag{4.7}$$

Remark 4.2. Clearly, if $\mathbf{U}$ is a weak solution of the variational equation $A(\mathbf{U},\mathbf{V}) = \ell(\mathbf{V})$ for all $\mathbf{V} \in \mathcal{H}^1$, then we can choose arbitrary q_N but $\mathbf{v} = 0$ and $q = 0$ in $\mathbf{V}$ such that the variational equation yields $(-\frac{1}{2}I + K)p = Vp_N$. In other words, p_N is the Neumann data of the exterior Helmholtz equation with Dirichlet data p. Using this and choosing $q_N = 0$ but arbitrary $\mathbf{v}$ and q in $\mathbf{V}$, classical arguments for the variational equation lead us to a solution $(\mathbf{u}, p)$ of the fluid-solid interaction in the interior with boundary data p and $\partial p/\partial n = p_N$ over Γ_D. Altogether we get a weak solution of (3.13)-(3.17) over the whole space. Similarly, it is easy to see that any weak solution $(\mathbf{u}, p)$ of (3.13)-(3.17) together with

$$p_N := V^{-1}\Big(-\frac{1}{2}I + K\Big)p$$

forms a solution of $A(\mathbf{U},\mathbf{V}) = \ell(\mathbf{V})$.

Remark 4.3. For the numerical solution, we proceed as in the previous remark. We choose finite element spaces $\mathcal{H}_h(\Omega) \subset (H^1(\Omega))^2$, $\mathcal{H}_h(\Omega_D) \subset H^1(\Omega_D)$, and $\mathcal{H}_h(\Gamma_D) \subset H^{-1/2}(\Gamma_D)$, and set $\mathcal{H}_h := \mathcal{H}_h(\Omega) \times \mathcal{H}_h(\Omega_D) \times \mathcal{H}_h(\Gamma_D)$. The finite element solution $\mathbf{U}_h \in \mathcal{H}_h$ is the solution of $A(\mathbf{U}_h,\mathbf{V}_h) = \ell(\mathbf{V}_h)$ for all $\mathbf{V}_h \in \mathcal{H}_h$. We obtain the usual stability and convergence results. In the practical computation, we first choose arbitrary $q_{N,h}$ but $\mathbf{v}_h = 0$ and $q_h = 0$ and solve $A(\mathbf{U}_h,(0,0,q_{N_h})) = \ell((0,0,q_N))$ with respect to $p_{N,h}$. This is of course the solution of $b((p_h,p_{N,h}),(0,q_{N,h})) = 0$, i.e., the solution of

$$\langle Vp_{N,h}, q_{N,h}\rangle = \Big\langle \Big(-\frac{1}{2}I_h + K_h\Big)p_h, q_{N,h}\Big\rangle.$$

In other words, $p_{N,h}$ is the SGBEM solution of the equation

$$Vp_N = \Big(-\frac{1}{2}I + K\Big)p, \ \textit{i.e.,}\ p_{N,h} = S_h p_h := V_h^{-1}\Big(-\frac{1}{2}I_h + K_h\Big)p_h$$

is the value of a discretized Dirichlet-to-Neumann operator applied to p_h. Stability and convergence for this first step are well established. Next we substitute this solution $p_{N,h}$ into the equation $A(\mathbf{U}_h,\mathbf{V}_h) = \ell(\mathbf{V}_h)$ and choose $q_{N,h} = 0$ but arbitrary $\mathbf{v}_h \in \mathcal{H}_h(\Omega)$ and $q_h \in \mathcal{H}_h(\Omega_D)$. This way we arrive at a new variational equation with classical terms over the domain but with a discretized Dirichlet-to-Neumann mapping in the term over Γ_D.

$$\widetilde{A}\big((\mathbf{u}_h,p_h),(\mathbf{v}_h,q_h)\big) = \ell\big((\mathbf{v}_h,q_h)\big), \quad \forall \mathbf{v}_h \in \mathcal{H}_h(\Omega), \forall q_h \in \mathcal{H}_h(\Omega_D), \tag{4.8}$$

$$\widetilde{A}\big((\mathbf{u}_h,p_h),(\mathbf{v}_h,q_h)\big) := a_1(\mathbf{u}_h,\mathbf{v}_h) + a_2(p_h,q_h) + a_3(\mathbf{u}_h,q_h) + a_4(p_h,\mathbf{v}_h) - \int_{\Gamma_D} S_h p_h \overline{q}_h.$$

Since this finite element method is obtained by eliminating the unknowns $p_{N,h}$ (Schur complement based on a stable subblock of the finite element matrix), stability and convergence for this method follows from the corresponding results for the variational equation over the full space $\mathcal{H}_h$ (cf. the subsequent Theorems 4.1–4.3 and the classical theory of finite element methods) and from those for the variational form $\langle Vp_{N,h}, q_{N,h}\rangle$. No extra estimate for the difference $S - S_h$, Dirichlet-to-Neumann mapping minus discretized Dirichlet-to-Neumann mapping, is needed.

In the following, we study the essential features of the variational equation (4.1).

Theorem 4.1. *The sesquilinear form $A(\mathbf{U},\mathbf{V})$ in (4.1) satisfies*

$$|A(\mathbf{U},\mathbf{V})| \le c\|\mathbf{U}\|_{\mathcal{H}^1}\|\mathbf{V}\|_{\mathcal{H}^1}, \quad \forall\, \mathbf{U},\mathbf{V} \in \mathcal{H}^1, \tag{4.9}$$

where c is the continuity constant independent of $\mathbf{U}$ and $\mathbf{V}$.

Proof. This continuity result is a direct consequence of the Cauchy-Schwarz inequality, the trace theorem and the boundedness of the DtN mapping S. □

Theorem 4.2. *The sesquilinear form* $A(\mathbf{U},\mathbf{V})$ *in* (4.1) *satisfies Gårding's inequality taking the form*

$$Re\,\{A(\mathbf{V},\mathbf{V})+(C\mathbf{V},\mathbf{V})_{\mathcal{H}^1}\}\geq\alpha\|\mathbf{V}\|^2_{\mathcal{H}^1},\quad\forall\,\mathbf{V}=(\mathbf{v},q)\in\mathcal{H}^1. \tag{4.10}$$

where $C:\mathcal{H}^1\to\mathcal{H}^1$ *is a compact operator and* $(\cdot,\cdot)_{\mathcal{H}^1}$ *denotes the inner product on* $\mathcal{H}^1$*. Here,* $\alpha>0$ *is a constant independent of* $\mathbf{V}$*.*

Proof. We first consider the sesquilinear form $a_1(\mathbf{v},\mathbf{v})$. It has been proved e.g. in [38] that there exist constants $\alpha,\beta>0$ independent of $\mathbf{v}$ satisfying Korn's inequality

$$Re\{a_1(\mathbf{v},\mathbf{v})\}\geq\alpha\,\|\mathbf{v}\|^2_{(H^1(\Omega))^2}-\beta\,\|\mathbf{v}\|^2_{(H^0(\Omega))^2}.$$

Therefore, there is a compact linear operator $C_1:(H^1(\Omega))^2\to(H^1(\Omega))^2$ defined by

$$(C_1\mathbf{u},\mathbf{v})_{(H^1(\Omega))^2}=\beta\int_\Omega\mathbf{u}\cdot\overline{\mathbf{v}}dx \tag{4.11}$$

such that

$$Re\{a_1(\mathbf{v},\mathbf{v})+(C_1\mathbf{v},\mathbf{v})_{(H^1(\Omega))^2}\}\geq\alpha\,\|\mathbf{v}\|^2_{(H^1(\Omega))^2}. \tag{4.12}$$

Similarly, for the sesquilinear form $a_2(q,q)$, since

$$\begin{aligned}a_2(q,q)&=\int_{\Omega_D}|\nabla q|^2\,dx-k^2\int_{\Omega_D}|q|^2dx\\&=\|q\|^2_{H^1(\Omega_D)}-(k^2+1)\,\|q\|^2_{H^0(\Omega_D)},\end{aligned}$$

we conclude that there is a compact linear operator $C_2:H^1(\Omega_D)\to H^1(\Omega_D)$ defined by

$$(C_2p,q)_{H^1(\Omega_D)}=(1+k^2)\int_{\Omega_D}p\overline{q}dx$$

such that

$$Re\{a_2(q,q)+(C_2q,q)_{H^1(\Omega_D)}\}\geq\|q\|^2_{H^1(\Omega_D)}. \tag{4.13}$$

Next, we consider the sesquilinear form $a_3(\mathbf{v},q)$. The Hölder inequality and the arithmetic-geometric mean inequality imply

$$\begin{aligned}|a_3(\mathbf{v},q)|&=\left|\rho_f\omega^2\int_\Gamma\mathbf{v}\cdot\mathbf{n}\,\overline{q}ds\right|\\&\leq\rho_f\omega^2\,\|\mathbf{v}\|_{(H^0(\Gamma))^2}\,\|q\|_{H^0(\Gamma)}\\&\leq\frac{\rho_f\omega^2}{2}\left(\|\mathbf{v}\|^2_{(H^0(\Gamma))^2}+\|q\|^2_{H^0(\Gamma)}\right).\end{aligned} \tag{4.14}$$

Then from the compact imbedding $H^{1/2}(\Gamma)\hookrightarrow L^2(\Gamma)$, we conclude that there exists a compact operator $C_3:\mathcal{H}^1\to\mathcal{H}^1$ such that

$$Re\Big\{a_3(\mathbf{v},q)+(C_3\mathbf{V},\mathbf{V})_{\mathcal{H}^1}\Big\}\geq 0. \tag{4.15}$$

Similarly, for the sesquilinear form $a_4(q, \mathbf{v})$, it follows that there exists a compact linear operator $C_4 : \mathcal{H}^1 \to \mathcal{H}^1$ such that

$$Re\Big\{a_4(q, \mathbf{v}) + (C_4\mathbf{V}, \mathbf{V})_{\mathcal{H}^1}\Big\} \geq 0. \tag{4.16}$$

Finally, we consider the quadratic form $b((q, q_N), (q, q_N))$. From the definition, we can see that

$$\begin{aligned} b\big((q, q_N), (q, q_N)\big) &= -2\,\langle Kq, \overline{q}_N\rangle_{\Gamma_D} + 2\,\langle Vq_N, \overline{q}_N\rangle_{\Gamma_D} \\ &\geq -\langle C_5 q, \overline{q}_N\rangle_{\Gamma_D} + c_6\|q_N\|^2_{H^{-1/2}(\Gamma_D)} - \langle C_6 q_N, \overline{q}_N\rangle_{\Gamma_D}\,, \end{aligned} \tag{4.17}$$

where $C_5 := 2K : \ H^{1/2}(\Gamma_D) \to H^{1/2}(\Gamma_D)$ is compact and where the constant c_6 and the compact operator $C_6 : \ H^{-1/2}(\Gamma_D) \to H^{1/2}(\Gamma_D)$ are taken from the well-known Gårding inequality for the single layer operator V. Combining the last estimate and (4.12)–(4.16), we get Gårding's inequality (4.10). □

As a consequence of Theorems 3.6 and 4.3, Fredholm's alternative leads us to

Theorem 4.3. *If* (a). *the surface* Γ *and the material parameters* (μ, λ, ρ) *are such that there are no traction free solutions, and* (b). *the artificial boundary* Γ_D *is such that* k *is not an exceptional value, then the variational equation* (4.1) *admits a unique solution.*

5. Numerical Schemes

Let $\widetilde{\mathcal{H}}_h \subset \widetilde{\mathcal{H}}^1 := \big(H^1(\Omega)\big)^2 \times H^1(\Omega_D)$ be a standard finite element space. Then the Galekin formulation of (4.1) reads: *Given* p^{inc} *and* $\partial p^{inc}/\partial n$, *find* $\mathbf{U}_h = (\mathbf{u}_h, p_h) \in \widetilde{\mathcal{H}}_h$, $\mathbf{u}_h = (u_1^h, u_2^h)$ *such that*

$$\widetilde{A}(\mathbf{U}_h, \mathbf{V}_h) = \ell(\mathbf{V}_h), \quad \forall\ \mathbf{V}_h = (\mathbf{v}_h, q_h) \in \widetilde{\mathcal{H}}_h. \tag{5.1}$$

In order to use FEM, the computational domains Ω and Ω_D are discretized by uniform triangular elements and we employ piecewise linear basis function $\{\varphi_i^{\Omega}\}_{i=1}^{N_1}$ in Ω and $\{\varphi_i^{\Omega_D}\}_{i=1}^{N_2}$ in Ω_D to construct the finite element space $\widetilde{\mathcal{H}}_h$. Here N_1 and N_2 are the total number of nodes in Ω and Ω_D, respectively, and we denote by $\{x_i\}_{i=1}^{N_1}$ and $\{y_i\}_{i=1}^{N_2}$ the nodes in Ω and Ω_D, respectively. Then we can derive a linear system

$$A_h\vec{X}_h = B_h, \quad A_h = \begin{bmatrix} A_1 & A_3 \\ A_4 & A_2 \end{bmatrix},$$

where $\vec{X}_h = (u_1^h(x_1), u_2^h(x_1), \ldots, u_1^h(x_{N_1}), u_2^h(x_{N_1}), p_h(y_1), \ldots, p_h(y_{N_2}))^T$ and the matrices $A_i, i = 1, \ldots, 4$ can be obtained according to the sesquilinear forms a_1, a_2+b, a_3 and a_4, respectively. In particular, we need to evaluate the terms $S\varphi_i^{\Omega_D}|\Gamma_D$, $i = 1, \ldots, N_2$. According to the representation of the DtN mapping S in (3.8), this amounts to solving the boundary integral equation of the first kind for σ on Γ_D in terms of $\mu = \varphi_i^{\Omega_D}|\Gamma_D$ in which $\varphi_i^{\Omega_D}|\Gamma_D$ does not vanish on Γ_D. In the following, we review three numerical methods for solving the boundary integral equation (3.8) and derive a simple formula for computing $b(p_h, q_h)$ if Γ_D is a circle.

5.1. SGBEM

The standard weak formulation of boundary integral equation (3.8) takes the form: *Given* $\mu \in H^{1/2}(\Gamma_D)$, *find* $\sigma \in H^{-1/2}(\Gamma_D)$ *such that*

$$B(\sigma, \chi) = f(\chi), \quad \forall \chi \in H^{-1/2}(\Gamma_D), \tag{5.2}$$

where $B(\sigma,\chi)=\langle\chi,V\sigma\rangle_{\Gamma_D}$ is a sesquilinear form on $H^{-1/2}(\Gamma_D)\times H^{-1/2}(\Gamma_D)$, $f(\chi)=\langle\chi,(-I/2+K)\mu\rangle_{\Gamma_D}$ is a linear functional on $H^{-1/2}(\Gamma_D)$, and $\langle\cdot,\cdot\rangle_{\Gamma_D}$ denotes the standard L^2 duality pairing on $H^{-1/2}(\Gamma_D)\times H^{1/2}(\Gamma_D)$.

In order to employ SGBEM, one needs to discretize the boundary Γ_D into element segments and replace the solution function space $H^{-1/2}(\Gamma_D)$ with the boundary element space $S_{Bh}\subset H^{-1/2}(\Gamma_D)$. Suppose that the boundary Γ_D is discretized into N segments $\Gamma_1,\Gamma_2,\ldots,\Gamma_N$ by nodes $x_1,x_2,\ldots,x_N$. Let $\{\psi_j\}_{j=1}^N$ be the basis of piecewise constant basis functions in S_{Bh} and $\{\varphi_j\}_{j=1}^N$ the basis of piecewise linear basis functions. We seek an approximate solution σ_h in the form

$$\sigma_h=\sum_{j=1}^{N}\sigma_j\psi_j, \tag{5.3}$$

where the $\sigma_j, j=1,\ldots,N$, are the unknown values of σ_h on the Γ_j. The given Dirichlet data μ is interpolated in the form

$$\mu=\sum_{j=1}^{N}\mu_j\varphi_j, \tag{5.4}$$

where $\mu_j, j=1,\ldots,N$, are the function values of μ at the end points x_j of the segments $\Gamma_j,\ j=1,\ldots,N$. Then we arrive at a linear system of equations

$$V_h\vec{\sigma}=\left(-\frac{1}{2}I_h+K_h\right)\vec{\mu}, \tag{5.5}$$

where $\vec{\sigma}=(\sigma_1,\ldots,\sigma_N)^T$, $\vec{\mu}=(\mu_1,\ldots,\mu_N)^T$ and V_h, I_h, K_h are matrices with entries

$$V_h(i,j)=\int_{\Gamma_D}V\psi_j\psi_i ds, \tag{5.6}$$

$$I_h(i,j)=\int_{\Gamma_D}\varphi_j\psi_i ds, \tag{5.7}$$

$$K_h(i,j)=\int_{\Gamma_D}K\varphi_j\psi_i ds. \tag{5.8}$$

It follows that the singular part with kernel behaviour $k(x,y)\sim|x-y|^{-1}$ in the entries $K_h(i,j)$ for $i=j$ or $i=j\pm1$ is exactly zero since $(x-y)\cdot\mathbf{n}_y=0$. The entries $V_h(i,i)$, $i=1,\ldots,N$ can be computed analytically by using the series expansion of the Hankel function $H_0^{(1)}(k|x-y|)$ [1], that is,

$$H_0^{(1)}(k|x-y|)=\sum_{m=0}^{\infty}\left[\left(C_m+D_m\ln\frac{k}{2}\right)k^{2m}|x-y|^{2m}+D_mk^{2m}|x-y|^{2m}\ln|x-y|\right],$$

where

$$C_m=\begin{cases}1+\frac{2ic_e}{\pi} & \text{if } m=0\\ \frac{(-1)^m}{2^{2m}m!m!}\left[1+\frac{2ic_e}{\pi}-\frac{2i}{\pi}\sum_{l=1}^{m}\frac{1}{l}\right] & \text{if } m\geq1,\end{cases}$$

$$D_m=\frac{2i(-1)^m}{\pi 2^{2m}m!m!},\quad m\geq0,$$

and c_e is the Euler constant. The remaining entries of the matrix V_h and K_h are calculated by using a Gauss quadrature rule.

We denote by G_h^S the projection for SGBEM defined as

$$G_h^S:\sigma\mapsto\sigma_h.$$

5.2. FMM based on variational formulation

The Galerkin boundary integral operators in (5.6) and (5.8) have kernels in terms of the fundamental solution of the Helmholtz equation and its normal derivative, respectively. These kernels are nonlocal functions which establish the relationship between the source point y and the field point x in the acoustic fields. The fast multipole method requires to factorize the Hankel function $H_0^{(1)}(k|x-y|)$ in order to realize an acceleration of the computations. As in Figure 5.1, for a fixed source point $y \in \Gamma_D$ and a fixed field point $x \in \Gamma_D$, we assume that $|z_1 - z_2| > |z_2 - x|$ and $|z_1 - z_2| > |z_1 - y|$, where $z_1, z_2 \in \Gamma_D$ are two points properly chosen nearby y and x, respectively.

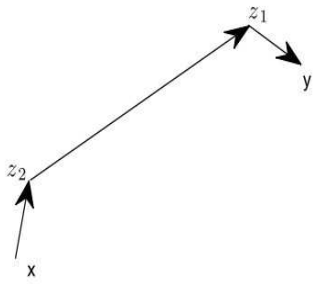

Fig. 5.1. Factorization of the Hankel function $H_0^{(1)}(k|x-y|)$.

An efficient factorization [5] of the Hankel function via Graf's addition formula [1] and the diagonalization of the translation operator lead to the representation

$$H_0^{(1)}(k|x-y|) \approx \frac{1}{2\pi} \int_0^{2\pi} \beta_{xz_2}(\alpha)\alpha_{z_2z_1}(\alpha)\beta_{z_1y}(\alpha)d\alpha, \tag{5.9}$$

where

$$\beta_{xz_2}(\alpha) = e^{-ik|z_2-x|\cos(\alpha-\phi_{xz_2})}, \tag{5.10}$$

$$\alpha_{z_2z_1}(\alpha) = \sum_{m=-P}^{P} H_m^{(1)}(k|z_1-z_2|)e^{-im(\phi_{z_2z_1}-\alpha+\frac{\pi}{2})}, \tag{5.11}$$

$$\beta_{z_1y}(\alpha) = e^{-ik|y-z_1|\cos(\alpha-\phi_{z_1y})} \tag{5.12}$$

are considered as functions of α. Here ϕ_{AB} is the angle between the vector $\overrightarrow{AB}$ and the positive x axis. Note that $\alpha_{z_2z_1}$ is a truncated series with expansion length P. This truncation is mandatory due to the fact that the summation diverges as P approaches ∞ since the value of the Hankel function increases quickly as the order m is larger than its argument $k|z_1 - z_2|$. On one hand, one expects to keep expansion length P as large as possible in order to obtain a satisfactory numerical accuracy. On the other hand, one anticipates to make the near field as small as possible where the SGBEM is employed for numerical computations. For interested readers, a discussion about the quantitative choice of P can be found in [35]. A practical equation for recommended values of P is

$$P = kl + c\log(kl + \pi),$$

where k is the wave number, l stands for the diameter of the source cluster group, and c is a constant dependent on the precision of the computer arithmetics. For the numerical evaluation

of the integral in (5.9), we employ the midpoint rule with a fixed number of quadrature points Q and obtain

$$H_0^{(1)}(k|x-y|)\approx\frac{1}{Q}\sum_{q=1}^{Q}\beta_{xz_2}(\alpha_q)\alpha_{z_2z_1}(\alpha_q)\beta_{z_1y}(\alpha_q). \tag{5.13}$$

While applying the FMM to solve the Galerkin formulation of (5.2), there are two kinds of errors. The first arises from the series truncation of the multipole expansion (5.11) and the second from the application of the numerical integral formula (5.13). Numerical examples in the next section show that such errors can be managed. Choosing the numerical parameters in the FMM appropriately the errors are negligible with respect to the numerical discretization errors of the FEM and BEM.

We now return to the FMM for the operators in (5.5). We present fast multipole computational formulas for the matrix-vector products in (5.5). For simplicity, we employ the mid-point quadrature rule for the evaluation of integrals in (5.6)–(5.8). Applying the factorization formula (5.13) and (5.6)–(5.8), we obtain the two-level fast multipole formulas for the i^{th} row of the matrix-vector product in $V_h\vec{\sigma}$ and $K_h\vec{\mu}$

$$(V_h\vec{\sigma})_i = \mathbf{NF} + \frac{i}{4Q}\Delta_i\beta^T_{x_iz_l}\cdot\sum_{G_{l'}\in G_l^{FF}}\alpha_{z_lz_{l'}}\cdot\sum_{y_j\in G_{l'}}\beta_{z_{l'}y_j}\Delta_j\sigma_j,$$

$$(K_h\vec{\mu})_i = \mathbf{NF} + \frac{i}{4Q}\Delta_i\beta^T_{x_iz_l}\cdot\sum_{G_{l'}\in G_l^{FF}}\alpha_{z_lz_{l'}}\cdot\sum_{y_k\in G_{l'}}(n_{y_k}\cdot\nabla_{y_k}\beta_{z_{l'}y_k})\Delta_k\sum_{j\in N(k)}\varphi_j|_k(x_k)\mu_j.$$

Here, **NF** indicates the total numerical data generated by the source points located in the near fields G_l^{NF} of the cluster $G_l = G_l^{NF}\cup G_l^{FF}$, where the collocation or field point x_i is located, and needs to be computed via the standard boundary element method, Δ_l is the Jacobian of the element Γ_l, $\varphi_j|_k$ is the linear basis function φ_j restricted to the element Γ_k, n_x is the unit normal vector pointing outward at the point x, $\nabla_x f$ is the gradient of f at the point x, $z_{l'}$ is the center of cluster group $G_{l'}$, $N(k)$ is the set of nodes related with the element Γ_k. Finally, we denote by G_h^F the Galerkin projection approximated by FMM as

$$G_h^F : \sigma \mapsto \sigma_h.$$

5.3. NM

Following the description of section 3.5 in [7], we recommend the NM based on product quadrature over an equidistant mesh and on trigonometric interpolation. Suppose that the smooth boundary curve Γ_D possesses a regular analytic and 2π-periodic parametric representation taking the form

$$x(t) = (x_1(t), x_2(t)), \quad 0\le t\le 2\pi,$$

in counterclockwise orientation satisfying $|x'(t)|^2 > 0$ for all t. Then we can transform (3.8) into the parametric form

$$\int_0^{2\pi} M(t,\tau)\psi(\tau)d\tau = -g(t) - \int_0^{2\pi} L(t,\tau)g(\tau)d\tau,$$

where $\psi(t) := \sigma(x(t))$, $g(t) := \mu(x(t))$ and the kernels are defined by

$$M(t,\tau) := \frac{i}{2} H_0^{(1)}(k|x(t)-x(\tau)|)|x'(\tau)|,$$
$$L(t,\tau) := \frac{ik}{2}\Big\{x_2'(\tau)[x_1(\tau)-x_1(t)] - x_1'(\tau)[x_2(\tau)-x_1(t)]\Big\}\frac{H_1^{(1)}(k|x(t)-x(\tau)|)}{|x(t)-x(\tau)|}$$

for $t \neq \tau$. Due to the logarithmic sigularities at $t = \tau$ of the kernels L and M, the kernels can be split into

$$M(t,\tau) := M_1(t,\tau)\ln\left(4\sin^2\frac{t-\tau}{2}\right) + M_2(t,\tau),$$
$$L(t,\tau) := L_1(t,\tau)\ln\left(4\sin^2\frac{t-\tau}{2}\right) + L_2(t,\tau),$$

where

$$M_1(t,\tau) := -\frac{1}{2\pi} J_0(k|x(t)-x(\tau)|)|x'(\tau)|,$$
$$M_1(t,t) := \left(\frac{i}{2} - \frac{c_e}{\pi} - \frac{1}{\pi}\ln\left(\frac{k}{2}|x'(t)|\right)\right)|x'(t)|,$$
$$L_1(t,\tau) := \frac{k}{2\pi}\Big(x_2'(\tau)[x_1(\tau)-x_1(t)] - x_1'(\tau)[x_2(\tau)-x_1(t)]\Big)\frac{J_1(k|x(t)-x(\tau)|)}{|x(t)-x(\tau)|}, \quad t \neq \tau,$$
$$L_2(t,t) = L(t,t) = \frac{x_1'(t)x_2''(t) - x_2(t)x_1''(t)}{2\pi|x'(t)|^2}.$$

Here, c_e is the Euler constant. Thus, via trigonometric quadrature rule and trapezoidal rule the solution of (3.8) reduces to solving a finite dimentional linear system. In particular, for any solution of (3.8) the values $\sigma_i^N = \psi(t_i^N), i = 0, 1, \ldots, N-1$ at the quadrature points $t_i^N = 2i\pi/N$ satisfy the linear system

$$\sum_{j=0}^{N-1}\left\{R_{|i-j|}^N M_1(t_i^N, t_j^N) + \frac{2\pi}{N} M_2(t_i^N, t_j^N)\right\}\sigma_i^N$$
$$= -g(t_i^N) - \sum_{j=0}^{N-1}\left\{R_{|i-j|}^N L_1(t_i^N, t_j^N) + \frac{2\pi}{N} L_2(t_i^N, t_j^N)\right\} g(t_j^N) \tag{5.14}$$

for $i = 0, 1, \ldots, N-1$ where

$$R_j^N := -\frac{4\pi}{N}\sum_{m=1}^{N/2-1}\frac{1}{m}\cos\frac{2mj\pi}{N} - \frac{4(-1)^j\pi}{N^2}, \qquad j = 0, 1, \ldots, N-1.$$

For the analysis of the NM and its application to other types of boundary integral equations in acoustic, we refer to [30]. Combining this with the FEM in numerical computations, which leads to the NM-FEM coupling procedure, we first compute the NM solution $\sigma_{i+1/2}^N$ at the points $t_{i+1/2}^N = 2(i+1/2)\pi/N$ and then define the solution $\sigma_h := \sigma_{i+1/2}^N$ over $I_i = [t_i^N, t_{i+1}^N)$ by constant interpolation. In this case, we denote the projection for NM as

$$G_h^N : \sigma \mapsto \sigma_h.$$

5.4. Computation of $b(\varphi_j^{\Omega_D}, \varphi_i^{\Omega_D})$ while Γ_D is a circle

Now set $\Gamma_D = \Gamma_R := \{x \in \mathbb{R}^2 : |x| = R\}$. In the discrete formulation, this amounts to computing the integrals

$$\int_{\Gamma_R} \left(S^h \varphi_j^{\Omega_D}\right) \overline{\varphi_i^{\Omega_D}} ds, \quad i,j = 1, \ldots, N_2. \tag{5.15}$$

In particular, we have to solve the boundary integral equations to determine

$$S^h \varphi_j^{\Omega_D} = G_h \circ V^{-1} \left(-\frac{1}{2} I + K\right) \varphi_j^{\Omega_D}, \quad j = 1, \ldots, N_2,$$

and then to compute the integral (5.15) using any appropriate quadrature rule.

As for our numerical computation, the finite element space consists of piecewise linear functions and most of them will vanish on the boundary Γ_R, thus reducing the complexity of the above mentioned part of the procedure. Even though, the computational task is formidable in the general case. Therefore, the fast and accurate evaluation of the boundary integral equation (5.15) is of great significance for the feasibility and improvement of the coupling method. In [32], the authors proposed a numerical procedure for the choice of the curve Γ_R and the corresponding finite element space S_h. More precisely, the restrictions of basis functions of S_h to Γ_R are piecewise linear functions of the arclength along Γ_R, which form the boundary element space $S_h \subset H^{1/2}(\Gamma_R)$.

Suppose that the first N_θ piecewise linear basis functions in $\{\varphi_i^{\Omega_D}\}_{i=1}^{N_2}$ do not vanish on Γ_R. In contrast to [32], the outer boundary Γ_R is not divided by equispaced nodes due to the unstructed partition for the computational domain. Suppose that Γ_D is now divided by N_θ nodes $x_1, x_2, \ldots, x_{N_\theta}$ and the j^{th} point $x_j, j = 1, \ldots, N_\theta$ possesses the polar coordinates (R, θ_j). Let $\Delta\theta_j$ be the angle between the line segments $0, x_j$ and $0, x_{j+1}$. Those $\varphi_j^{\Omega_D}$'s which do not vanish on Γ_R can be denoted, using the same symbols, by

$$\varphi_j^{\Omega_D}(\theta) = \begin{cases} \frac{\theta - \theta_{j-1}}{\Delta\theta_{j-1}}, & \theta_{j-1} \le \theta \le \theta_j, \\ \frac{\theta_{j+1} - \theta}{\Delta\theta_j}, & \theta_j \le \theta \le \theta_{j+1}, \\ 0, & others. \end{cases}$$

We define

$$\tilde{\psi}_j(\theta) = \begin{cases} 1 + \frac{\theta}{\Delta\theta_{j-1}}, & -\Delta\theta_{j-1} \le \theta \le 0, \\ 1 - \frac{\theta}{\Delta\theta_j}, & 0 \le \theta \le \Delta\theta_j, \\ 0, & -\pi \le \theta \le -\Delta\theta_{j-1}, \Delta\theta_j \le \theta \le \pi, \end{cases}$$

and extend this to a 2π-periodic function $\tilde{\psi}_j(\theta)$ such that $\varphi_j^{\Omega_D}(\theta) = \tilde{\psi}_j(\theta - \theta_j)$. We first expand the function $\tilde{\psi}_j(\theta)$ into a Fourier series

$$\tilde{\psi}_j(\theta) = \frac{a_0}{2} + \sum_{k=1}^{\infty} (a_k \cos k\theta + b_k \sin k\theta),$$

where for $k \geq 1$,

$$
\begin{aligned}
a_0 &= \frac{\Delta\theta_{j-1} + \Delta\theta_j}{2\pi}, \\
a_k &= \frac{1}{\pi k^2}\left(\frac{1-\cos k\Delta\theta_{j-1}}{\Delta\theta_{j-1}} + \frac{1-\cos k\Delta\theta_j}{\Delta\theta_j}\right), \\
b_k &= \frac{1}{\pi k^2}\left(\frac{\sin k\Delta\theta_{j-1}}{\Delta\theta_{j-1}} - \frac{\sin k\Delta\theta_j}{\Delta\theta_j}\right).
\end{aligned}
$$

Note that, by solving elementary boundary value problems for the circle, one obtains for $n = 0, 1, 2, \ldots$,

$$
S\Big(\cos(n(\theta+\alpha))\Big) = \frac{kH_n^{(1)'}(kR)}{H_n^{(1)}(kR)}\cos(n(\theta+\alpha)),
$$

where $H_n^{(1)}(kR)$ is the Hankel function of the first kind of order n. Then after some algebraic rearrangements, we arrive at the explicit approximate formula for the integral (5.15) of the form

$$
\begin{aligned}
&\int_{\Gamma_R} (S^h\varphi_j^{\Omega_D})\overline{\varphi_i^{\Omega_D}}\,ds \\
&\approx \frac{kRH_0^{(1)'}(kR)(\Delta\theta_{i-1}+\Delta\theta_i)(\Delta\theta_{j-1}+\Delta\theta_j)}{8\pi H_0^{(1)}(kR)} \\
&\quad + \frac{R}{\pi}\left(\frac{1}{\Delta\theta_{i-1}} + \frac{1}{\Delta\theta_i}\right)\left(\frac{1}{\Delta\theta_{j-1}} + \frac{1}{\Delta\theta_j}\right) S^h(\rho)(\theta_i - \theta_j) \\
&\quad - \frac{R}{\pi}\left(\frac{1}{\Delta\theta_{i-1}} + \frac{1}{\Delta\theta_i}\right)\left[\frac{S^h(\rho)(\theta_i - \theta_j + \Delta\theta_{j-1})}{\Delta\theta_{j-1}} + \frac{S^h(\rho)(\theta_i - \theta_j - \Delta\theta_j)}{\Delta\theta_j}\right] \\
&\quad - \frac{R}{\pi}\left(\frac{1}{\Delta\theta_{j-1}} + \frac{1}{\Delta\theta_j}\right)\left[\frac{S^h(\rho)(\theta_i - \theta_j + \Delta\theta_{i-1})}{\Delta\theta_{i-1}} + \frac{S^h(\rho)(\theta_i - \theta_j - \Delta\theta_i)}{\Delta\theta_i}\right] \\
&\quad + \frac{R}{\pi}\left[\frac{S^h(\rho)(\theta_i - \theta_j - \Delta\theta_{i-1} + \Delta\theta_{j-1})}{\Delta\theta_{j-1}\Delta\theta_{i-1}} + \frac{S^h(\rho)(\theta_i - \theta_j + \Delta\theta_i + \Delta\theta_{j-1})}{\Delta\theta_{j-1}\Delta\theta_i}\right] \\
&\quad + \frac{R}{\pi}\left[\frac{S^h(\rho)(\theta_i - \theta_j - \Delta\theta_{i-1} - \Delta\theta_j)}{\Delta\theta_j\Delta\theta_{i-1}} + \frac{S^h(\rho)(\theta_i - \theta_j + \Delta\theta_i - \Delta\theta_j)}{\Delta\theta_j\Delta\theta_i}\right],
\end{aligned}
$$

where

$$
\rho(\theta) = \frac{\pi^4}{90} - \frac{\pi^2\theta^2}{12} + \frac{\pi\theta^3}{12} - \frac{\theta^4}{48}. \tag{5.16}
$$

Consequently, to evaluate all the integrals (5.15), one simply needs to compute the values of $S^h\rho$ on Γ_R for the single function $\rho(\theta)$ in (5.16). This leads us to solve the boundary integral equation with the numerical solution

$$
S^h(\rho) = G_h \circ V^{-1}\Big(-\frac{1}{2}I + K\Big)\rho, \tag{5.17}
$$

for $G_h = G_h^S$ (or G_h^F, G_h^N). We denote by N the number of nodes on Γ_R for solving (5.17).

6. Numerical Experiments

In this section, we present the results of several numerical tests by employing BIE-based DtN-FEM. In particular, we call this method SGBEM-FEM, FMM-FEM and NM-FEM if we

use SGBEM, FMM and NM, respectively, to solve the boundary integral equation (3.8). To evaluate the accuracy of the numerical solution, we consider a model problem with $p^{inc} = e^{ikx_1}$ and $\Omega = \{x \in \mathbb{R}^2 : |x| < R_0\}$. The exact solution of (2.1)–(2.5) is given in [38]. The linear systems generated for each method are solved by GMRES without the use of preconditioners and the iteration is terminated as the relative residual is below 10^{-5}.

Example 6.1. In order to test the codes of SGBEM, FMM and NM, we first separately consider the numerical treatment of (3.8) with $\mu = -e^{ikx_1}$. We choose $R = 2$ and the wave number $k = 1$. In Table 6.1, we can see that the FMM provides the same order of accuracy as SGBEM (see 1st and 2nd column) and the approximation error of NM decreases exponentially (see 3rd column). Considering the complexity with respect to the degrees of freedom N over the boundary curve Γ_D only, the two-level FMM is more advantageous over the SGBEM and NM as N increases. The actual complexities for SGBEM, NM and two-level FMM are $O(N^2)$, $O(N^2)$ and $O(N^{3/2})$, respectively. Note that the NM for the separated example is the best method since, for a fixed prescribed accuracy, it requires the smallest number of degrees of freedom N. Unfortunately, employing the NM for the coupling leads to right-hand sides including piecewise linear trial functions of the FEM part such that the analyticity assumption for the exponential convergence of the NM are not satisfied anymore. Therefore, complexity should be counted as a function of N. Choosing the number of degrees of freedom N in the size of the dimension of the FEM space restricted to Γ_D, the L^2-error of $G_h^N\sigma$ becomes asymptotically the same as SGBEM as N increases.

Table 6.1: Numerical errors of three numerical methods for the boundary integral equation (3.8).

N	SGBEM (L^2-error)	FMM (L^2-error)	NM (l^∞-error)
4	1.85E0	1.91E0	5.35E-1
8	1.00E0	1.00E0	4.43E-2
16	5.11E-1	5.26E-1	6.23E-5
32	2.56E-1	2.65E-1	5.89E-13
64	1.28E-1	1.32E-1	1.61E-14

Next, we consider the fluid-solid interaction problem. We choose Γ and Γ_D to be circles with radius R_0 and R, respectively. We are going to apply the coupling procedures SGBEM-FEM, FMM-FEM and NM-FEM for solving the fluid-solid interaction problem (2.1)–(2.5). In the following, we take the parameters $\omega = 1$, $\mu = 1$, $\lambda = 1$, $\rho = 1$, $\rho_f = 1$, $R_0 = 1$ and $R = 2$. Note that the formulation presented in section 5.4 for computing $b(\varphi_j^{\Omega_D}, \varphi_i^{\Omega_D})$ can be used. On the other hand, one can first use SGBEM, FMM and NM to compute all the $\sigma_h^j = S^h\varphi_j^{\Omega_D}$ on the boundary elements of Γ_i, $i = 1, 2, \cdots, N$, for which $\varphi_j^{\Omega_D}$ does not vanish on Γ_D, and then take the arithmetic average of $S^h\varphi_j^{\Omega_D}$ to give its value on the boundary elements of the finite element mesh. The integral $\int_{\Gamma_R} \sigma_h^j \overline{\varphi_i^{\Omega_D}}\, ds$ is calculated by Gauss quadrature rule to approximate $b(\varphi_j^{\Omega_D}, \varphi_i^{\Omega_D})$. We call this procedure P-II and the one described at the end of Subsection 5.4 P-I.

Example 6.2. In this example, we first choose $N = 4N_\theta$. This implies that the boundary Γ_R is discretized into $4N_\theta$ boundary elements for the computation formula (5.17). Fig. 6.1 and 6.2 show the the log-log plot of errors measured in $\widetilde{\mathcal{H}}^0$ and $\widetilde{\mathcal{H}}^1$-norms with respect to $1/h_F$, respectively, considering $k = 1, 2$ and 4 for P-I, where h_F is the finite element meshsize. Slopes

of -2 in Fig. 6.1(a,b,c) and -1 in Fig. 6.2(a,b,c) verify the convergence order of $O(h_F^2)$ and $O(h_F)$ which indicate the optimal convergence rate

$$\|\mathbf{U}-\mathbf{U}_h\|_{\widetilde{\mathcal{H}}^t}=O(h_F^{2-t}),\quad t=0,1. \tag{6.1}$$

To investigate the interaction between the finite element meshsize h_F and the boundary element meshsize h_B and to obtain the optimal order of accuracy, we choose $k=2$, $N=N_\theta,2N_\theta,4N_\theta$. It can be seen from Fig. 6.3 and 6.4 that if the number N is not sufficiently large, the numerical errors for large finite element meshsize can still be reduced and the performance of the convergence order is larger than the standard.

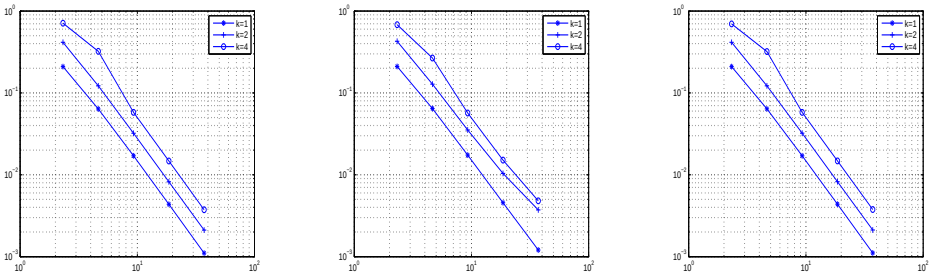

(a) (b) (c)

Fig. 6.1. Log-log plots for numerical errors (vertical) of $\mathbf{U}$ for P-I in $\mathcal{H}^0$-norm vs. $1/h_F$ (horizontal) when $N=4N_\theta$. (a): SGBEM-FEM; (b): FMM-FEM ; (c): NM-FEM.

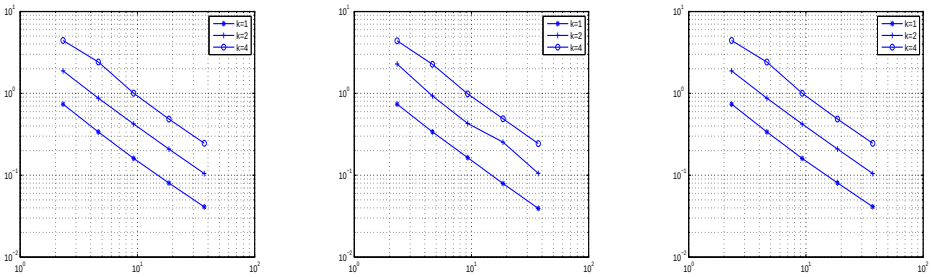

(a) (b) (c)

Fig. 6.2. Log-log plots for numerical errors (vertical) of $\mathbf{U}$ for P-I in $\mathcal{H}^1$-norm vs. $1/h$ (horizontal) when $N=4N_\theta$. (a): SGBEM-FEM; (b): FMM-FEM ; (c): NM-FEM.

Example 6.3. We consider P-II in this example and present the log-log plot of errors measured in $\widetilde{\mathcal{H}}^0$ and $\widetilde{\mathcal{H}}^1$-norms with respect to $1/h_F$ considering $k=1,2$ and 4 in Fig. 6.5 and 6.6. The numerical results also illustrated the optimal convergence rate (6.1).

Example 6.4. Note that the artificial boundary Γ_D can be chosen flexibly. For a general shape of the elastic body, one can choose an appropriate Γ_D close to Γ to reduce the size of the computation domain. In this case, P-I is not available. So, in the last example, we

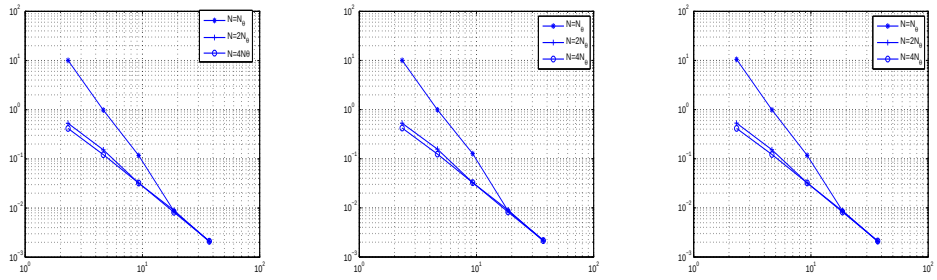

(a) (b) (c)

Fig. 6.3. Log-log plots for numerical errors (vertical) of $\mathbf{U}$ for P-I in $\mathcal{H}^0$-norm vs. $1/h$ (horizontal) when $k = 2$. (a): SGBEM-FEM; (b): FMM-FEM ; (c): NM-FEM.

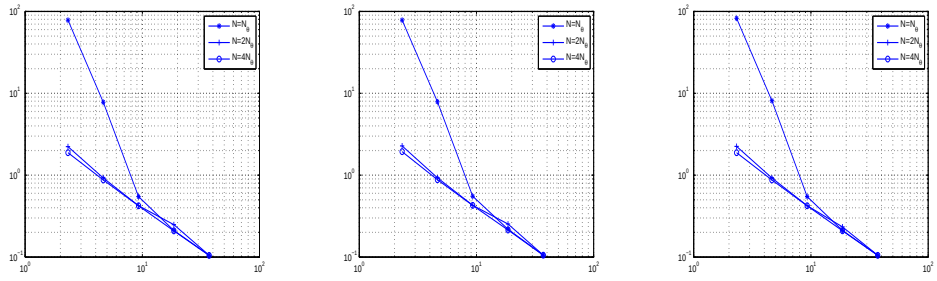

(a) (b) (c)

Fig. 6.4. Log-log plots for numerical errors (vertical) of $\mathbf{U}$ for P-I in $\mathcal{H}^1$-norm vs. $1/h$ (horizontal) when $k = 2$. (a): SGM-FEM; (b): FMM-FEM ; (c): NM-FEM.

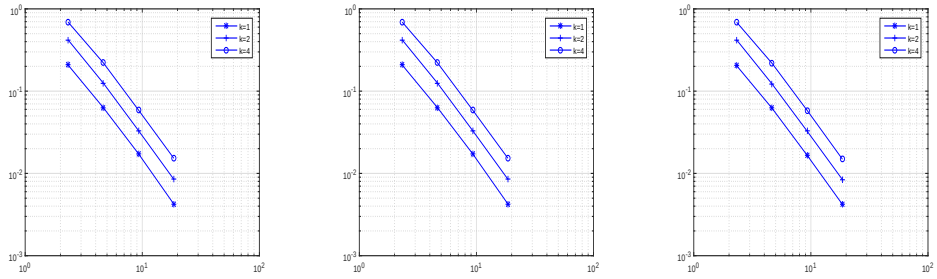

(a) (b) (c)

Fig. 6.5. Log-log plots for numerical errors (vertical) of $\mathbf{U}$ for P-II in $\mathcal{H}^0$-norm vs. $1/h$ (horizontal) when $N = 4N_\theta$. (a): SGBEM-FEM; (b): FMM-FEM ; (c): NM-FEM.

consider a water-brass interaction problem (in mm level). The frequency and speed of sound are $\omega = \pi \times 10^6$ Hz and $c_0 = 1480$ m/s, and the density of water is $\rho_f = 1000$ kg/m^3. The density of brass is $\rho = 8100$ kg/m^3. The velocities for shear waves and pressure waves are $c_s = 2270$ m/s and $c_p = 4840$ m/s, respectively. Assume that Γ now is curved-triangle-shaped

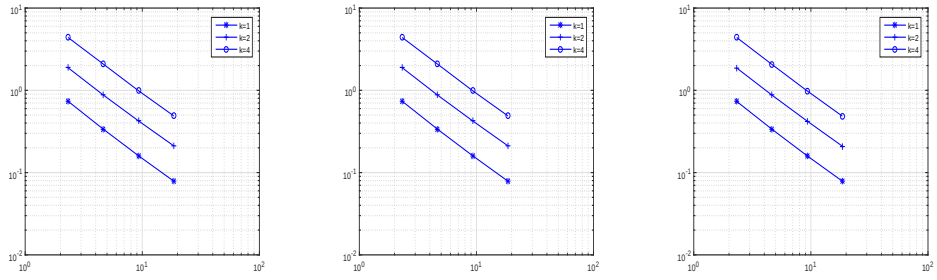

(a) (b) (c)

Fig. 6.6. Log-log plots for numerical errors (vertical) of $\mathbf{U}$ for P-II in $\mathcal{H}^1$-norm vs. $1/h$ (horizontal) when $N = 4N_\theta$. (a): SGBEM-FEM; (b): FMM-FEM ; (c): NM-FEM.

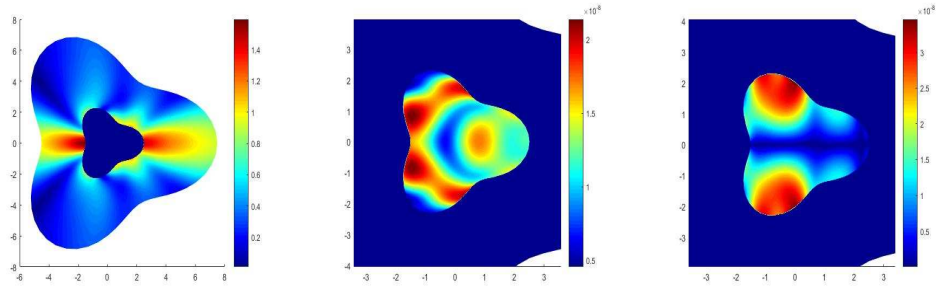

(a) $|u_1|$ (b)$|u_2|$ (c)$|p|$

Fig. 6.7. Numerical solution of a water-brass interaction problem.

characterized by $\{(\theta, r(\theta)) : \theta \in [0, 2\pi)\}$ where

$$r(\theta) := 2 + 0.5\cos 3\theta \quad \text{mm}, \quad \theta \in [0, 2\pi),$$

and we choose Γ_D as a bigger curved-triangle-shaped and smooth curve close to Γ. We set $N = 4N_\theta$ and present the numerical solutions based on NM-FEM in Fig. 6.7. As shown there, our coupling procedures apply even to more general problems. Note that, in most cases of practical engineering, the fluid-solid interaction couples fields with large differences in their magnitudes.

Acknowledgments. The work of T. Yin is partially supported by the NSFC Grant (11371385). The work of L. Xu is partially supported by the NSFC Grant (11371385), the Start-up fund of Youth 1000 plan of China and that of Youth 100 plan of Chongqing University.

References

[1] M. Abramowitz, I.A. Stegun, Handbook of mathematical functions, Dover Publ., New York, 1972.
[2] J. Bérenger, A perfectly matched layer for the absorption of electromagnetic waves, *J. Comput. Phys.*, **114** (1994), 185-200.
[3] R.A. Bustinza, G.N. Gatica, F.-J. Sayas, A look at how LDG and BEM can be coupled, *ESAIM Proceedings*, **21** (2007), 88-97.

[4] J. Bielak, R.C. MacCamy, Symmetric finite element and boundary integral coupling methods for fluid-solid interaction, *Q. Appl. Math.*, **49** (1991), 107-119.
[5] W. Chew, J. Jin, E. Michielssen, J. Song, Fast and Efficient Algorithms in Computational Electromagnetics, Artech House, 2001.
[6] D. Colton, R. Kress, Integral equation methods in scattering theory, John Wilery and Sons, New York, 1983.
[7] D. Colton, R. Kress, Inverse Acoustic and Electromagnetic Scattering Theory, Springer, Berlin, 2013.
[8] C. Domínguez, E.P. Stephan, M. Maischak, A FE-BE coupling for a fluid-structure interaction problem: hierarchical a posteriori error estimates, *Numer. Methods Partial Differential Equations*, **28** (2012), 1417-1439.
[9] C. Domínguez, E.P. Stephan, M. Maischak, FE/BE coupling for an acoustic fluid-structure interaction problem. Residual a posteriori error estimates, *Internat. J. Numer. Methods Engrg.*, **89** (2012), 299-322.
[10] S. Engleder, O. Steinbach, Stabilized boundary element methods for exterior Helmholtz problems, *Numer. Math.*, **110** (2008), 145-160.
[11] J.J. Faran, Sound scattering by solid cylinders and spheres, *J. Acoust. Soc. Amer.*, **23(5)** (1951), 405-418.
[12] K. Feng, Finite element method and natural boundary reduction, in: Proceedings of the International Congress of Mathematicians, Warsaw, 1983, 1439-1453.
[13] D. Givoli, Numerical Methods for Problems in Infinite Domains, Academic Press, Elsevier, 1992.
[14] G.N. Gatica, G.C. Hsiao, S. Meddahi, A residual-based a posteriori error estimator for a two-dimensional fluid-solid interaction problem, *Numer. Math.*, **114** (2009), 63-106.
[15] G.N. Gatica, A. Márquez, S. Meddahi, Analysis of the coupling of primal and dual-mixed finite element methods for a two-dimensional fluid-solid interaction problem, *SIAM J. Numer.Anal.*, **45(5)** (2007), 2072-2097.
[16] G.N. Gatica, A. Márquez, S. Meddahi, Analysis of the coupling of BEM, FEM and mixed-FEM for a two-dimensional fluid-solid interaction problem, *Appl. Numer. Math.*, **59(11)** (2009), 2735-2750.
[17] H. Han, X. Wu, Artificial boundary method, Springer-Verlag Berlin Heidelberg, 2013.
[18] R. Hiptmair, P. Meury, Stabilized fem-bem coupling for Helmholtz transmission problems, *SIAM J. Numer. Anal.*, **44** (2006), 2107-2130.
[19] C.O. Horgan, Korn's Inequalities and their Applications in Continuum Mechanics, *SIAM Review*, **37(4)** (1995), 491-511.
[20] G.C. Hsiao, On the boundary-field equation methods for fluid-structure interactions, *Problems and methods in mathematical physics* (Chemnitz, 1993), 79C88, Teubner-Texte Math., 134, Teubner, Stuttgart, 1994.
[21] G.C. Hsiao, Boundary element methods-An overview, *Appl. Numer. Math.*, **56** (2006), 1356-1369.
[22] G.C. Hsiao, F. Liu, J. Sun, L. Xu, A coupled BEM and FEM for the interior transmission problem in acoustics, *J. Comput. Appl. Math.*, **235** (2011), 5213-5221.
[23] G.C. Hsiao, N. Nigam, J.E. Pasciak, Li. Xu, Error analysis of the DtN-FEM for the scattering problem in acoustics via Fourier analysis, *J. Comput. Appl. Math.*, **235** (2011), 4949-4965.
[24] G.C. Hsiao, W. Wendland, Boundary element methods: foundation and error analysis, in: E. Stein, R. de Borst, T.J.R. Hughes (Eds.), in: Encyclopedia of Computational Mechanics, vol. 1, John Wiley and Sons, Ltd., 2004, 339-373.
[25] G.C. Hsiao, W.L. Wendland, Boundary Integral Equations, Springer-verlag, 2008.
[26] G.C. Hsiao, L. Xu, A system of boundary integral equations for the transmission problem in acoustics, *Appl. Numer. Math.*, **61** (2011), 1017-1029.
[27] G.C. Hsiao, R.E. Kleinman, G.F. Roach, Weak solutions of fluid-solid interaction problems, *Math. Nachr.*, **218** (2000), 139-163.
[28] G. Hu, A. Rathsfeld, T. Yin, Finite element method for fluid-solid interaction problem with

unbounded perioidc interfaces, *Numer. Methods Partial Differential Equations*, **32** (2016), 5-35.

[29] D.S. Jones, Low-frequency scattering by a body in lubricated contact, *Quart. J. Mech. Appl. Math.*, **36** (1983), 111-137.

[30] R. Kress, On the numerical solution of a hypersingular integral equation in scattering theory, *J. Comput. Appl. Math.*, **61** (1995), 345-360.

[31] C.J. Luke, P.A. Martin, Fluid-solid interaction: acoustic scattering by a smooth elastic obstacle, *SIAM J. Appl. Math.*, **55(4)** (1995), 904-922.

[32] R.C. MacCamy, S.P. Marin, A Finite Element Method for Exterior Interface Problems, *Internat. J. Math. Math. Sci.*, **3(2)** (1980), 311-350.

[33] A. Márquez, S. Meddahi, V. Selgas, A new BEM-FEM coupling strategy for two-dimensionam fluid-solid interaction problems, *J. Comput. Phys.*, **199** (2004), 205-220.

[34] D. Nicholls, N. Nigma, Exact non-reflecting boundary conditions on general domains, *J. Comput. Phys.*, **194** (2004), 278-303.

[35] N. Nishimura, Fast multipole accelerated boundary integral equation methods, *Appl. Mech. Rev.*, **55** (2002), 299-324.

[36] V. Rokhlin, Rapid solution of integral equation of scattering theory in two dimensions, *J. Comput. Phys.*, **86** (1990), 414-439.

[37] W.I. Wendland, On asymptotic error estimates for the combined BEM and FEM, in: E. Stein, W.L. Wendland(eds.), Finite Element and Boundary Element techniques from mathematical and engineering point of view, CISM Lec-ture Notes 301, Udine, Springer-Verlag, Wien-New York, 273-333, 1988.

[38] T. Yin, L. Xu, A priori error estimates of the Fourier-series-based DtN-FEM for fluidstructure interaction problem, submitted.

[39] T. Yin, G.C. Hsiao, L. Xu, Boundary integral equation method for the fluid-solid interaction problems, submitted.